JOC The Journal of Organic Chemistry

pubs.acs.org/joc Article

Inclusion-Activated Reversible *E*/*Z* Isomerization of a Cyanostilbene Derivative Based on Cucurbit[8]uril under 365 nm Ultraviolet Irradiation

Xiaohan Sun, Zhixue Liu, Ze Wang, Man Huo, Heng-Yi Zhang,* and Yu Liu*

Cite This: https://doi.org/10.1021/acs.joc.2c00185 Read Online

ACCESS | Metrics & More | Article Recommendations | Supporting Information

ABSTRACT: The photoisomerization behavior of cyanostilbene molecules is a hotspot in supramolecular configuration transformation research. Here, we reported a cyanostilbene derivative that converted from the *Z*,*Z*-isomer to the *E*,*E*-isomer under UV light irradiation at 365 nm. This process can be reversibly converted only in the presence of cucurbit[8]uril under the same light source, accompanied by the reversible conversion of fluorescence from green to yellow. No effective configuration transformation occurred with guest molecules only or upon the addition of cucurbit[7]uril. The photoisomerization was fully characterized by UV−vis and fluorescence spectroscopy, NMR, high-resolution mass spectrometry, and transmission electron microscopy. This work provides a new method for the supramolecular macrocyclic-activated configuration transformation.

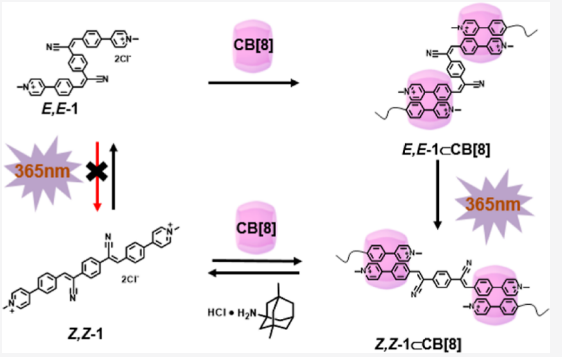

INTRODUCTION

The phenomenon of *E*/*Z* isomerism is ubiquitous in molecules with double bonds, but *Z*- and *E*-isomers usually have different properties, especially for the biological activity,[1] luminous state,[2] and topological morphology.[3] Until now, carbon−carbon double bonds,[4−6] imines, and azobenzene[7,8] have been widely used in photoisomerization of supramolecular topography control,[9] and many studies have been reported for the photoisomerization between different configurations under the stimulation of light or heat.[10,11]

Cyanostilbene molecules, as a commonly used photoisomerization group, not only contain double bonds that can carry out the isomerization process but also enable aggregation-induced emission because of the existence of cyano groups.[12−14] Therefore, the isomerization of the carbon−carbon double bond in cyanostilbene will make the change of the fluorescence spectrum more obvious. Recently, Tang and co-workers reported a cyanostilbene-based molecule that underwent different isomerization reactions under room light or ultraviolet light at 365 nm.[15] The conversion of *Z*/*E* isomers is commonly achieved by heating or lighting at different wavelengths. In addition, Zhao and co-workers connected the naphthalimide and quantum dots to the cyanostilbene moiety through an alkyl chain to obtain photoisomerization systems and mainly studied the luminescence state of cyanostilbene molecules in different configurations.[16,17] The above-mentioned research studies made a great contribution to the understanding of *E*/*Z* isomerization. However, for some molecules with double bonds, the isomerization rate is slow and time-consuming.[18] Therefore, it is worth studying to realize isomerization quickly and easily by lighting because of it simple, convenient, and controllable.

On the other hand, one possible additional strategy for accomplishing this task is to take advantage of supramolecular macrocyclic compounds,[19−22] especially cucurbit[*n*]uril (CB[*n*]).[23−25] CB[*n*] can bond positively charged guest molecules to form host−guest complexes in a process of dynamic equilibrium through non-covalent interactions.[26] In the previous reports, supramolecular macrocyclic host molecules were mostly used to research dimerization of double bonds to accelerate the reaction speed.[27,28]

Recently, we found that the CB[*n*]-based supramolecular system not only can facilitate the efficient inclusion of guest molecules but also activate the photoisomerization process of the *Z*- and *E*-isomers. Herein, we synthesized a cyanostilbene derivative (*Z*,*Z*-**1**), whose configuration can be changed from the *Z*,*Z*-isomer to the *E*,*E*-isomer under UV light irradiation at 365 nm (Scheme 1). Interestingly, the *E*,*E*-isomer cannot be converted back to the *Z*,*Z*-isomer, which can only be realized by the host−guest interaction of CB[8] under the same light source. Under irradiation with 365 nm UV light, the aggregate morphology of the *E*,*E*-isomer changes from nanofibers to

Received: January 26, 2022

Scheme 1. Schematic Diagram of Macrocyclic Regulation of *E*/*Z* Heterogeneity (Counterion: Cl^-)

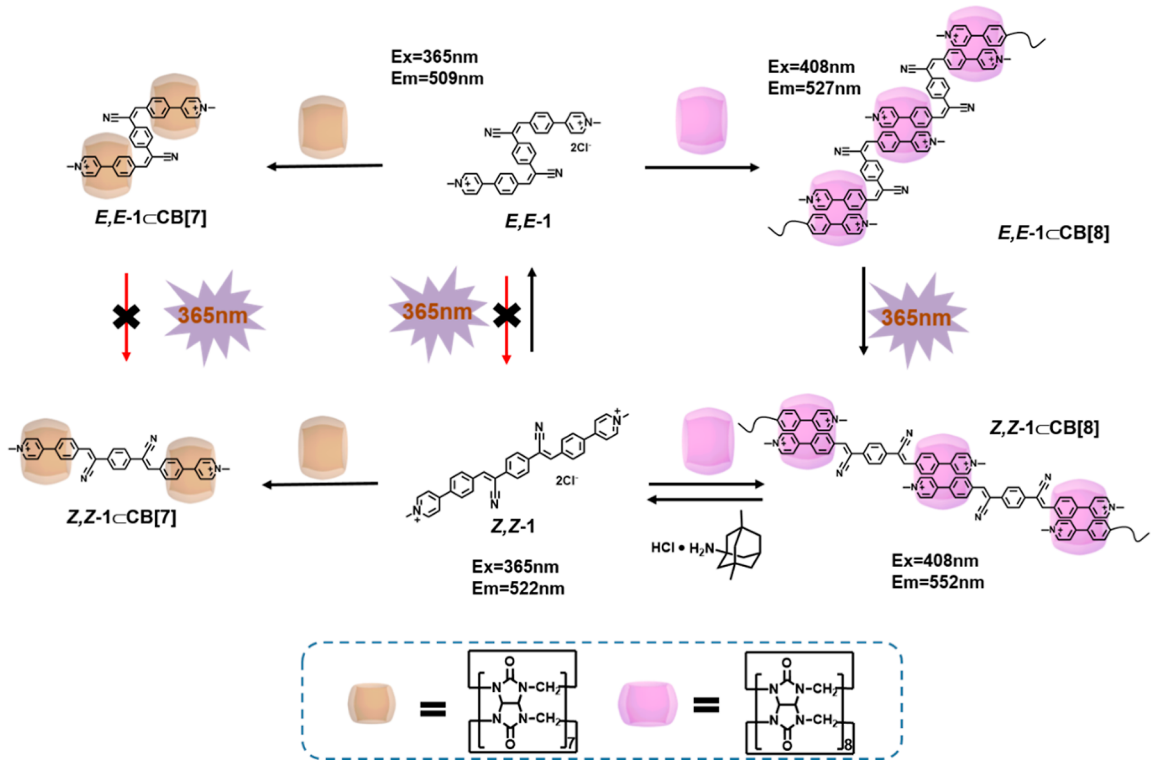

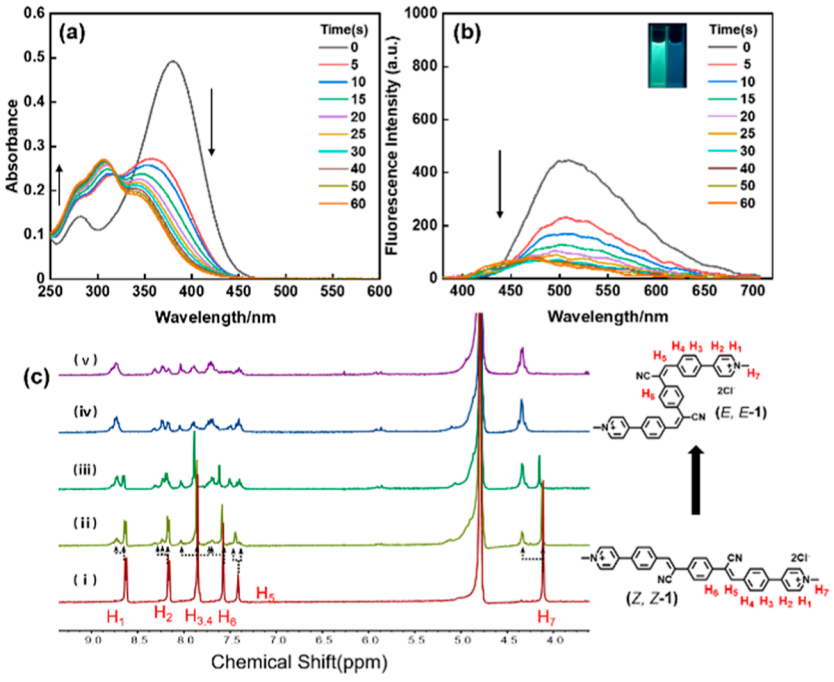

Figure 1. (a) UV−vis absorption and (b) fluorescence spectra of *Z*,*Z*-**1** (10 μM) in H_2O irradiated with 365 nm UV light from a UV lamp (6 W) for different times (0−60 s). (c) ^1H NMR spectra of *Z*,*Z*-**1** (1.0 mM) before (i) and after (ii−iv) UV−vis irradiation for (ii) 5, (iii) 15, and (iv) 25 min in D_2O and (v) spectra after heating at 80 °C for 24 h in D_2O using a metal mantle. λ_{ex} = 365 nm. Inset: fluorescence emission before (left) and after (right) UV irradiation under 365 nm light (counterion: Cl^-).

nanofragments and then forms nanosheets through host−guest interactions in the presence of CB[8]. Furthermore, these nanosheets can be converted back to nanofibers under UV light irradiation at 365 nm. High-resolution mass spectrometry (HRMS) and NMR tests demonstrate that this process is photoisomerization rather than photodimerization. As a comparison, CB[7] can also assemble with *Z*,*Z*-**1** but cannot facilitate configuration reversal from the *E*,*E*-isomer to the *Z*,*Z*-isomer. This work could provide a new strategy for the supramolecular macrocyclic-activated configuration switch of cyanostilbene derivatives under the same light source.

https://doi.org/10.1021/acs.joc.2c00185
J. Org. Chem. XXXX, XXX, XXX−XXX

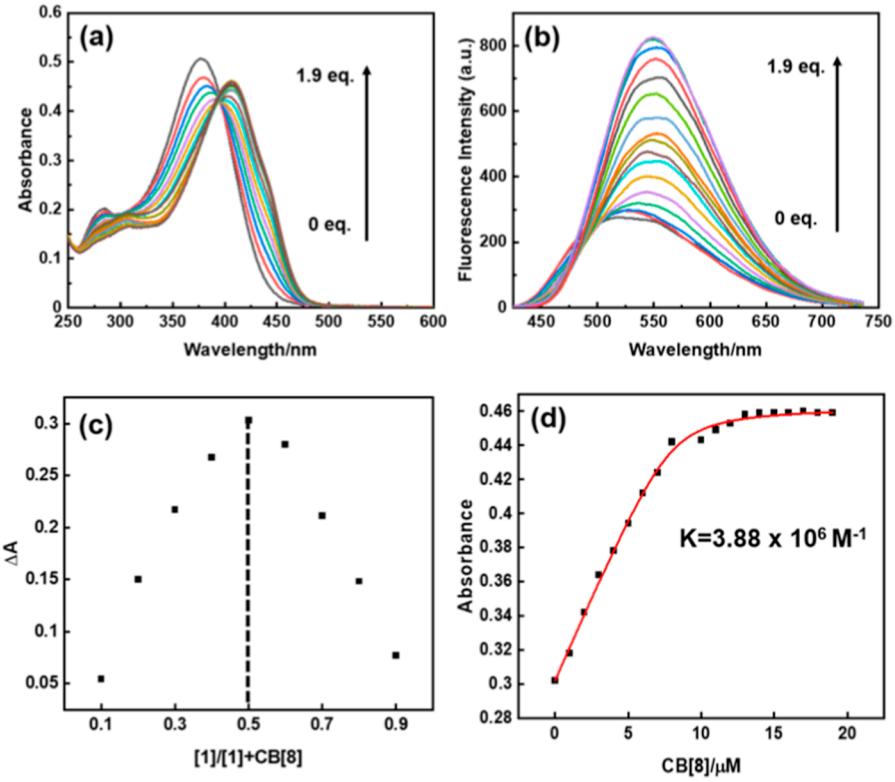

Figure 2. (a) UV−vis absorption and (b) fluorescence spectral changes of *Z,Z*-**1**⊂CB[8] (10 μM) upon addition of CB[8] in H_2O. λ_{ex} = 408 nm. (c) Job's plot of *Z,Z*-**1**⊂CB[8]. (d) Binding constant of *Z,Z*-**1**⊂CB[8].

RESULTS AND DISCUSSION

First, we synthesized a cyanostilbene derivative (*Z,Z*-**1**), which can perform *E*/*Z* isomerization under 365 nm UV light.[29−31] It is well known that molecules with double bonds can undergo dimerization, cyclization,[32,33] and isomerization reactions under ultraviolet light. Hence, we used UV−vis absorption and fluorescence spectroscopy to investigate the *E*/*Z* isomerization process (Figure 1).

In the initial state, *Z,Z*-**1** had two absorption peaks (380 and 281 nm) and a strong green fluorescence at 509 nm in aqueous solution. Under UV light irradiation at 365 nm, the absorption peak at 380 nm decreased gradually, accompanied by a 35 nm blue shift, and the absorption peak at 305 nm increased at the same time (Figure 1a). After 60 s of illumination at 365 nm, this peak almost disappeared. The same change also occurred in fluorescence spectroscopy. Its emission at 509 nm was gradually decreased, and it only displayed the emission at 470 nm, accompanied by the fluorescent color change from green to blue (Figure 1b). From the above-mentioned results, we deduced that *Z,Z*-**1** may be transformed into *E,E*-**1**. We curiously noticed that there were the very large changes in the first 5 s followed by a slower change over a longer timescale during this process. To explain reasonably this observation, we obtained the reaction rate and the half-life $t_{1/2}$ of the photoisomerization reaction. The chemical reaction rate was related to the reaction order, so the data at 380 nm in Figure 1a were used to study the relationship between the UV absorption value and reaction time according to the first-order reaction rate formula: $\ln[(A_\infty - A_0)/(A_\infty - A)] = kt$. As shown in Figure S2, $\ln[(A_{60} - A_0)/(A_{60} - A)]$ was well proportional to the change of reaction time, indicating that the photoisomerization reaction of *Z,Z*-**1** was a first-order reaction, and its $t_{1/2}$ = 7.95 s. Therefore, the reaction rate changed very fast in the first 5 s and then decreased greatly with the progress of the reaction.

Next, we used ^{1}H NMR and HRMS to test and verify the photoisomerization process. Figure 1c shows the conversion of the *Z,Z*-isomer to the *E,E*-isomer at different irradiation times by ^{1}H NMR. Signals corresponding to the aromatic protons (H_1−H_4, H_6) moved to the low field. However, the signals of protons on double bonds (H_5) had a completely opposite change and moved to a high field. The chemical shift of H_7 could obviously reveal the isomerization process of double bonds. The peak for H_7 at 4.11 ppm was weakened, and a new peak was generated at 4.34 ppm. Through the above-mentioned results, we confirmed that the configuration of *Z,Z*-**1** had changed. However, it was obvious that the ^{1}H NMR spectra of *Z,Z*-**1** were clear, but the spectra of *E,E*-**1** were weak and broad. The reason may come from the aggregation of *E,E*-**1** in aqueous solution. Meanwhile, Figure 1a shows that the spectra between 5 and 60 s of irradiation had a clear distinct isosbestic point, and the spectrum of the reactant (0 s) to the subsequent spectra showed the absence of an isosbestic point. The results further confirmed that once the photochemistry proceeds, the part of *Z,Z*-**1** changed to the *E,E*-**1** isomer, and the photoisomerization process was changed due to the self-aggregation of the *E,E*-**1** isomer. Subsequently, HRMS was selected to exclude the cyclization and dimerization of compounds. It was found that the mass-nucleus ratio of *Z,Z*-**1** did not change before and after illumination, which can rule out cyclization (Figure S3). Because *Z,Z*-**1** had two charges, the highest peak of isomerization was the same as with dimerization. However, the intervals between the peaks adjacent to the highest peak were different. The isomerization product only had two charges in one molecule, and its interval

https://doi.org/10.1021/acs.joc.2c00185
J. Org. Chem. XXXX, XXX, XXX−XXX

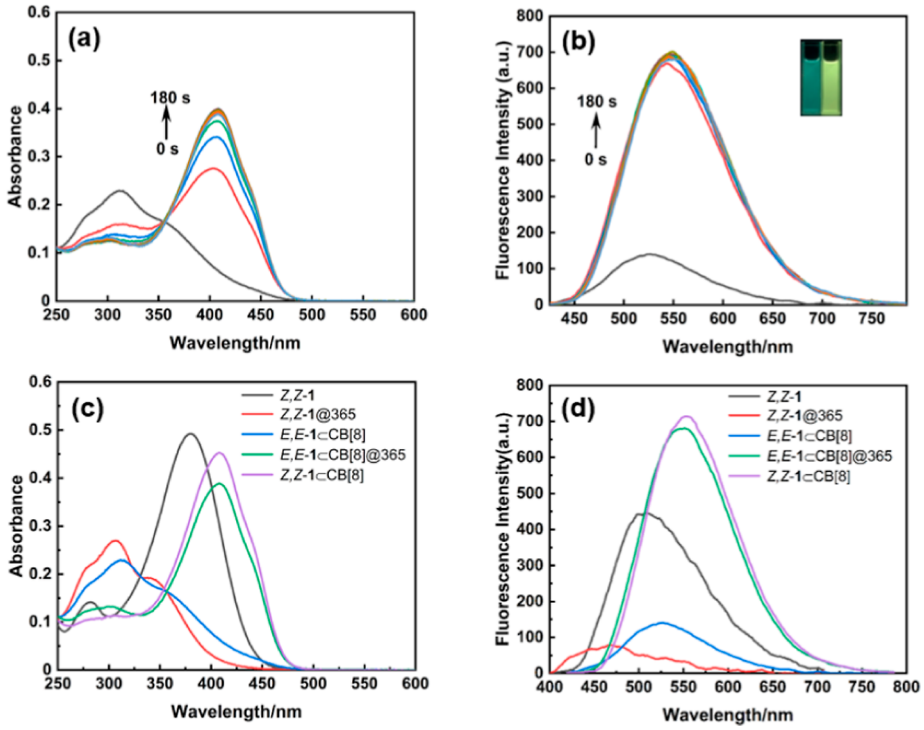

Figure 3. (a) UV−vis absorption and (b) fluorescence spectra of *E,E*-**1**⊂CB[8] ([*E,E*-**1**] = [CB[8]] = 10 μM) in H_2O irradiated with 365 nm UV light from a UV lamp (6 W) for different times. Inset: fluorescence emission before (left) and after (right) UV irradiation under 365 nm light. λ_{ex} = 408 nm. (c) UV−vis absorption and (d) fluorescence spectra of the *E*/*Z* isomerization process.

should be 0.5, and the [2 + 2] dimerization product had four charges in one molecule, and its interval should be 0.25. Before and after UV light irradiation at 365 nm, the intervals were 0.5, which was in accord with the isomerization reaction. Compared with the *E,E*-isomer, H_6 and H_5 of the *Z,Z*-isomer had closer distance in space. Fortunately, we found the signals of H_5 and H_6 on 2D nuclear overhauser effect spectroscopy (Figure S4a). For the *E,E*-isomer, the inversion of the double bond configuration kept H_5 away from H_6, and H_4 was close to H_6 (Figure S4b), which confirmed well the isomerization reaction. However, the massy H signal generated after UV light irradiation may also contain a small amount of *Z,E*-**1** and *E,Z*-**1** isomers. This result can also be confirmed by the UV−vis spectra, which showed a broad peak at 345 nm, implying the presence of *Z,E*-**1** and *E,Z*-**1** isomers (Figure 1a). After this, we tried to recover the configuration from the *E,E*-isomer to the *Z,Z*-isomer by heating. However, the results showed that heating had a very slight effect on the configurational change and made very little change on the NMR spectroscopy (Figure 1c).

To the best of our knowledge, CB[8] and positively charged guest molecules can form host−guest complexes through non-covalent interactions in a process of dynamic equilibrium. Hence, we deduced that this dynamic supramolecular system was conducive to the photoisomerization process. We first tested the assembly behavior between *Z,Z*-**1** and CB[8] to investigate the binding ratio. As shown in Figure 2a,b, after adding different concentrations of CB[8], the absorption peak at 380 nm was red-shifted by 30 nm. The fluorescence intensity continued increasing with the addition of CB[8], accompanied by a 30 nm red shift. These red shifts were due to the confinement effect of CB[8] which would restrict the movement of molecules and then change their luminescence. In addition, the binding ratio of *Z,Z*-**1**⊂CB[8] was 1:1 by Job's plot, and the binding constant was calculated to be 3.88×10^6 M^{-1} (Figure 2c,d).

Subsequently, CB[8] was added in the solution of *E,E*-**1** to obtain *E,E*-**1**⊂CB[8] assembly. Under UV light irradiation at 365 nm, a new absorption peak appeared at 408 nm with a gradual increase in intensity, while the absorption peak at 310 nm gradually decreased (Figure 3a). Meanwhile, the fluorescence intensity of *E,E*-**1**⊂CB[8] at 520 nm was increased, accompanied by a 30 nm red shift (Figure 3b). After illumination at 365 nm for 180 s, the fluorescence of *E,E*-**1**⊂CB[8] at 550 nm was the same as that of *Z,Z*-**1**⊂CB[8] in the initial state, and UV−vis absorption spectroscopy showed the same result (Figure S5). From the above-mentioned results, we can deduce that the *E,E*-**1** configuration can return to *Z,Z*-**1** in the presence of CB[8]. These observations indicated that the same light source could achieve the configuration switch of *E,E*-**1** mediated by CB[8]. In addition, ^{1}H NMR was used to further evaluate this change (Figure S6). After illumination at 365 nm in the presence of CB[8], the signal peaks of *E,E*-**1**⊂CB[8] reappeared but only displayed three peaks (Figure S6c). It was obvious that the spectra of *Z,Z*-**1**⊂CB[8] were the same as those of *E,E*-**1**⊂CB[8]@365 nm, confirming that the structures of *Z,Z*-**1**⊂CB[8] and *E,E*-**1**⊂CB[8]@365 nm were consistent (Figure S7). Because the binding between *Z,Z*-**1** and CB[8] was a dynamic process and it was a fast process on the NMR timescale, we could still compare the spectra by peak shapes and peak shifts, although the aromatic signal in ^{1}H NMR was weak and broad. From the above-mentioned results, we confirmed that the transformation of *E,E*-**1**⊂CB[8] was changed to *Z,Z*-**1**⊂CB[8] (Figure 3c,d). In addition, we studied the role of 365 nm light in this recovery process. *E,E*-**1**⊂CB[8] displayed no obvious change in the

https://doi.org/10.1021/acs.joc.2c00185
J. Org. Chem. XXXX, XXX, XXX−XXX

absorption and fluorescence spectra after 1 h without illumination (Figure S8).

In addition, we changed CB[8] to CB[7] to compare the effects of different assembly modes on the photoisomerization process. Job's plot of *E,E*-**1**⊂CB[7] showed that the binding ratio was 1:2, which was different from that of *E,E*-**1**⊂CB[8] due to the smaller cavity of CB[7] (Figure S9). The absorption peak red-shifted from 380 to 388 nm with a slight decrease in intensity. In addition, it was found that the fluorescence emission wavelength did not change, but the fluorescence intensity increased 2 times compared with *E,E*-**1** (Figure S10). The binding constants were $K_1 = 2.77 \times 10^5$ M^{-1} and $K_2 = 1.94 \times 10^6$ M^{-1} (Figure S11). Under UV light irradiation at 365 nm, the absorption peak at 315 nm was slightly decreased, and the peak at 361 nm was increased (Figure S12a). However, the fluorescence intensity was only recovered by half (Figure S12b). Although there was a tendency to reverse the transformation, the change was very small after 120 s illumination, and it was still a large difference from the initial state. Therefore, the photoisomerization process of *E,E*-**1** could not be realized by using CB[7].

TEM was used to study the morphological change during the *Z*/*E* photoisomerization process (Figure 4). All the photoisomerization tests were carried out in water, and the samples were decomposed into TEM samples for testing at different time points. The initial state was *Z,Z*-**1** without irradiation, and it showed a very obvious filamentous shape (Figure 4a). After light irradiation at 365 nm for 60 s, the filamentous shape changed to many small fragments which meant that the molecular structure was changed to form the *E,E*-isomer (Figure 4b). Then, we added CB[8] to the solution of *E,E*-**1** to obtain *E,E*-**1**⊂CB[8]. The small fragments of *E,E*-**1** were changed to large sheet structures (Figure 4c). Upon continuing to illuminate *E,E*-**1**⊂CB[8] for another 180 s, the assembly changed back to filamentous again (Figure 4d), while the topography was the same as that of *Z,Z*-**1**⊂CB[8] (Figure S13a). Through this morphological change of this *E*/*Z* isomerism process, we can confirm that the *E,E*-isomer can return to the *Z,Z*-isomer in the presence of CB[8]. In contrast, the morphology of *Z,Z*-**1**⊂CB[7] showed many irregular tiny fibrous fragments (Figure S13b), while the morphology of *Z,Z*-**1**⊂CB[8] displayed many linear assemblies. The different morphology might also come from the different inclusion modes between the host and the guest. In this system, CB[8] could bind *Z,Z*-**1** to form stable linear assemblies based on the binding ratio of 1:1, while CB[7] could only bind two *Z,Z*-**1** based on the binding ratio of 1:2, which was not conducive to forming a linear assembly. In addition, the fluorescence lifetime and quantum yield are also tested in Figure S14 and Table S1.

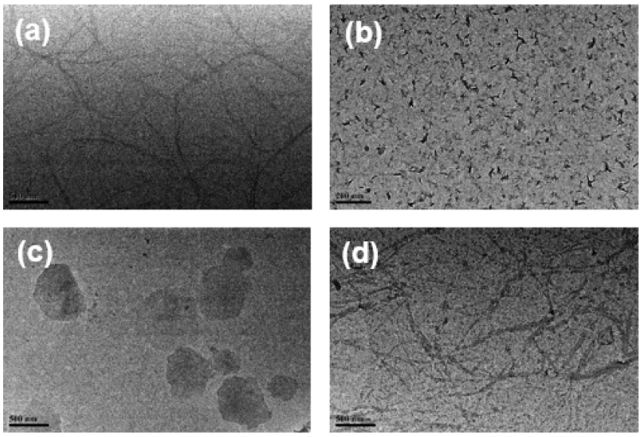

Figure 4. TEM images of (a) *Z,Z*-**1** without irradiation, (b) *E,E*-**1**, (c) *E,E*-**1**⊂CB[8], and (d) *E,E*-**1**⊂CB[8] after irradiation. (The scale bars are 500 nm in the TEM images.)

To compare the effect of CB[8] and CB[7] on the photoisomerization process, we analyzed the photoisomerization process between *Z,Z*-**1**⊂CB[8] and *Z,Z*-**1**⊂CB[7] (Figure S15). Under UV light irradiation at 365 nm, no obvious changes were found in UV−vis absorption and fluorescence spectra for the *Z,Z*-**1**⊂CB[8] assembly (Figure S15a,b). It was demonstrated that *Z,Z*-**1**⊂CB[8] was very stable in a light irradiation environment, proving that the addition of CB[8] makes *Z,Z*-**1** more stable in the *Z,Z*-isomer state. However, the *Z,Z*-**1**⊂CB[7] assembly exhibited obvious changes in both UV−vis absorption and fluorescence spectra, accompanied by a blue shift in UV absorption spectra and fluorescence intensity quenching, which was the same as the photoisomerization process of *Z,Z*-**1** (Figure S15c,d). This result suggested that CB[7] cannot effectively immobilize molecules in a single conformational state, such as the *Z*-isomer, and thus was not as effective as CB[8] in controlling the photoisomerization process. One reasonable explanation was that the confinement of macrocyclic molecules had a more obvious effect on *Z,Z*-**1**⊂CB[8] than CB[7], and the guest molecules were more stable in the *Z* configuration in the CB[8] cavity. Therefore, different supramolecular assemblies displayed different control effects during the photoisomerization process. When the assembly was exposed to 365 nm light, guest molecules were more inclined to keep in the *Z* configuration in the cavities of CB[8].

After this, we used 3,5-dimethyl-1-adamantylamine·HCl (Me_2ADA), which had a larger binding constant with CB[8],[34] to replace the guest molecules from assemblies (Figure S16). Upon addition of Me_2ADA to the solution of *Z,Z*-**1**⊂CB[8] and *E,E*-**1**⊂CB[8]@365 nm, both of them showed the same decrease in the absorption peak at 408 nm, accompanied by the increase in the absorption peak at 380 nm, which were the same as the absorption peaks of *Z,Z*-**1**. The above-mentioned results showed that we can replace *Z,Z*-**1** isomers by guest competition in the solution of *E,E*-**1**⊂CB[8] @365 nm and realize the complete recovery of *Z,Z*-**1** isomers.

CONCLUSIONS

In conclusion, we synthesized a cyanostilbene derivative (*Z,Z*-**1**), in which the configuration can be changed from the *Z,Z*-isomer to the *E,E*-isomer under UV light irradiation at 365 nm. Importantly, *E,E*-isomers cannot be converted back to *Z,Z*-isomers but can be realized through the host−guest interaction mediated by CB[8]. First, after UV light irradiation at 365 nm for 60 s, the shape of the *E,E*-isomer changed from nanofibers to nanofragments. Subsequently, upon the addition of CB[8] to form *E,E*-**1**⊂CB[8], these nanofragments can assemble together to form nanosheets through host−guest interaction. Finally, these nanosheets can be converted back to nanofibers under UV light irradiation at 365 nm for only 20 s. This process underwent a configuration change of the cyanostilbene derivative from the *E,E*-isomer to the *Z,Z*-isomer. HRMS and ^{1}H NMR further demonstrated this photoisomerization process rather than photodimerization. On the other hand, CB[7] can also assemble with *Z,Z*-**1** but cannot facilitate

https://doi.org/10.1021/acs.joc.2c00185
J. Org. Chem. XXXX, XXX, XXX−XXX

configuration reversal from the *E,E*-isomer to the *Z,Z*-isomer. Comparative experiments showed that only CB[8] can activate the conformational change from the *E,E*-isomer to the *Z,Z*-isomer. Therefore, CB[8] can not only include the molecules effectively but also activate supramolecular configuration change of cyanostilbene derivatives under the same light source, which provided a new strategy for activating *E*/*Z* isomerization.

EXPERIMENTAL SECTION

Preparation of Compound 2.

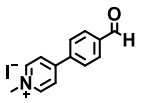

2

4-(4-Formylphenyl)pyridine (1.000 g, 5.458 mmol) was dissolved in iodomethane (0.854 g, 6.0038 mmol) and heated at 80 °C for 12 h using a metal mantle. After cooling to room temperature, the reaction mixture was filtered and washed with CH_3CN and diethyl ether. Yield (1.23 g, 66%). ^{1}H NMR (400 MHz, DMSO-d_6): δ 10.16 (s, 1H), 9.10 (d, J = 6.8 Hz, 2H), 8.59 (d, J = 6.9 Hz, 2H), 8.28 (d, J = 8.3 Hz, 2H), 8.15 (d, J = 8.4 Hz, 2H), 4.37 (s, 3H). ^{13}C{^{1}H} NMR (100 MHz, DMSO-d_6): δ 193.3, 153.3, 146.3, 139.1, 138.2, 130.7, 129.4, 125.3, 48.0. HRMS-ESI (m/z): calcd for $C_{13}H_{12}NO$ [M^+], 198.0914; found, 198.0916.

Preparation of Compound *Z,Z*-1 (2I$^-$).

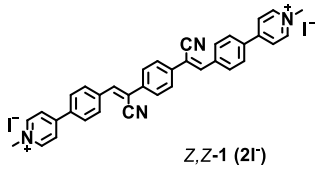

***Z,Z*-1 (2I$^-$)**

Tetrabutylammonium hydroxide (TBAH, 10 drops, 25%) was added to a solution of p-phenylenediacetonitrile (119.39 mg, 0.765 mmol) and compound **2** (500 mg, 1.683 mmol) in methanol (20 mL), and then, the reaction mixture was stirred at 80 °C for 12 h using a metal mantle. After cooling, the mixture was filtered, and the solid was washed with diethyl ether. Yield (355.12 mg, 60%). ^{1}H NMR (400 MHz, DMSO-d_6): δ 9.07 (d, J = 6.7 Hz, 4H), 8.59 (d, J = 6.8 Hz, 4H), 8.35 (s, 2H), 8.30 (d, J = 8.5 Hz, 4H), 8.21 (d, J = 8.5 Hz, 4H), 8.01 (s, 4H), 4.36 (s, 6H). ^{13}C{^{1}H} NMR (100 MHz, DMSO-d_6): δ 153.4, 146.2, 1426, 137.3, 135.5, 134.9, 130.7, 129.1, 127.2, 124.7, 117.9, 111.9, 47.7. HRMS-ESI (m/z): calcd for $C_{36}H_{28}N_4$ [M^{2+}], 258.1152; found, 258.1155.

Ion Exchange.

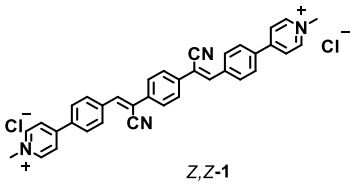

***Z,Z*-1**

Z,Z-**1** (2I$^-$) (200.00 mg, 0.264 mmol) was added to a 3000 mL beaker. Water was then added and stirred until the solid was completely dissolved. An excess of ammonium hexafluorophosphate was added, and a large amount of solid was produced. The system was filtered, and the solid was transferred to a 1000 mL beaker. After adding acetone and stirring to dissolve, excess tetrabutylammonium chloride was added, and a large amount of orange solid was produced. The system was filtered, the filtrate was discarded, and the solid was washed with acetone. Yield (87.20 mg, 57.14%). ^{1}H NMR (400 MHz, D_2O, ppm): δ 8.64 (d, J = 6.4 Hz, 4H), 8.17 (d, J = 6.4 Hz, 4H), 7.85 (d, J = 3.3 Hz, 8H), 7.57 (s, 4H), 7.40 (s, 2H), 4.12 (s, 6H).

ASSOCIATED CONTENT

Supporting Information

The Supporting Information is available free of charge at https://pubs.acs.org/doi/10.1021/acs.joc.2c00185.

Spectra data, HRMS, 2D NMR spectra, Job's plots, quantum yield and lifetime, TEM image, and compound characterization (PDF)

AUTHOR INFORMATION

Corresponding Authors

Heng-Yi Zhang − *College of Chemistry, State Key Laboratory of Elemento-Organic Chemistry, Nankai University, Tianjin 300071, P. R. China*; Email: hyzhang@nankai.edu.cn

Yu Liu − *College of Chemistry, State Key Laboratory of Elemento-Organic Chemistry, Nankai University, Tianjin 300071, P. R. China*; orcid.org/0000-0001-8723-1896; Email: yuliu@nankai.edu.cn

Authors

Xiaohan Sun − *College of Chemistry, State Key Laboratory of Elemento-Organic Chemistry, Nankai University, Tianjin 300071, P. R. China*

Zhixue Liu − *College of Chemistry, State Key Laboratory of Elemento-Organic Chemistry, Nankai University, Tianjin 300071, P. R. China*

Ze Wang − *College of Chemistry, State Key Laboratory of Elemento-Organic Chemistry, Nankai University, Tianjin 300071, P. R. China*

Man Huo − *College of Chemistry, State Key Laboratory of Elemento-Organic Chemistry, Nankai University, Tianjin 300071, P. R. China*

Complete contact information is available at: https://pubs.acs.org/10.1021/acs.joc.2c00185

Author Contributions

X.S. performed all experiments, wrote the main article, and prepared the figures. Z.L. and Z.W. tested the TEM and NMR. M.H. tested the fluorescence lifetimes and quantum yields. H.-Y.Z. and Y.L. supervised the work and edited the manuscript. All authors analyzed and discussed the results. All authors reviewed the manuscript.

Notes

The authors declare no competing financial interest.

ACKNOWLEDGMENTS

This work was supported by the National Natural Science Foundation of China (grant numbers 21772100, 21807038, and 22131008) and by the China Postdoctoral Science Foundation (grant number 2019M651006).

REFERENCES

(1) Bisby, R. H.; Botchway, S. W.; Hadfield, J. A.; McGown, A. T.; Parker, A. W.; Scherer, K. M. Fluorescence Lifetime Imaging of E-

combretastatin Uptake and Distribution in Live Mammalian Cells. *Eur. J. Cancer* **2012**, *48*, 1896−1903.
(2) Yu, W.; Zhang, H.; Yin, P.-A.; Zhou, F.; Wang, Z.; Wu, W.; Peng, Q.; Jiang, H.; Tang, B. Z. Restriction of Conformation Transformation in Excited State: An Aggregation-Induced Emission Building Block Based on Stable Exocyclic C=N Group. *iScience* **2020**, *23*, 101587.
(3) Sun, H.-L.; Chen, Y.; Han, X.; Liu, Y. Tunable Supramolecular Assembly and Photoswitchable Conversion of Cyclodextrin/Diphenylalanine-Based 1D and 2D Nanostructures. *Angew. Chem., Int. Ed.* **2017**, *56*, 7062−7065.
(4) Simeth, N. A.; Altmann, L.-M.; Wössner, N.; Bauer, E.; Jung, M.; König, B. Photochromic Indolyl Fulgimides as Chromo-pharmacophores Targeting Sirtuins. *J. Org. Chem.* **2018**, *83*, 7919−7927.
(5) Dang, H. T.; Nguyen, V. D.; Haug, G. C.; Vuong, N. T. H.; Arman, H. D.; Larionov, O. V. Z-Selective Dienylation Enables Stereodivergent Construction of Dienes and Unravels a Ligand-Driven Mechanistic Dichotomy. *ACS Catal.* **2021**, *11*, 1042−1052.
(6) Guerrin, C.; Szalóki, G.; Berthet, J.; Sanguinet, L.; Orio, M.; Delbaere, S. Indolino-Oxazolidine Acido- and Photochromic System Investigated by NMR and Density Functional Theory Calculations. *J. Org. Chem.* **2018**, *83*, 10409−10419.
(7) Saint-Louis, C. J.; Warner, D. J.; Keane, K. S.; Kelley, M. D.; Meyers, C. M.; Blackstock, S. C. Photo-Electroswitchable Arylaminoazobenzenes. *J. Org. Chem.* **2021**, *86*, 11341−11353.
(8) Constantin, C.-P.; Sava, I.; Damaceanu, M.-D. Structural Chemistry-Assisted Strategy toward Fast Cis−Trans Photo/Thermal Isomerization Switch of Novel Azo-Naphthalene-Based Polyimides. *Macromolecules* **2021**, *54*, 1517−1538.
(9) Sun, H.-L.; Chen, Y.; Zhao, J.; Liu, Y. Photocontrolled Reversible Conversion of Nanotube and Nanoparticle Mediated by beta-Cyclodextrin Dimers. *Angew. Chem., Int. Ed.* **2015**, *54*, 9376−9380.
(10) Kim, D.; Pillon, G.; DiPrimio, D. J.; Holland, P. L. Highly Z-Selective Double Bond Transposition in Simple Alkenes and Allylarenes through a Spin-Accelerated Allyl Mechanism. *J. Am. Chem. Soc.* **2021**, *143*, 3070−3074.
(11) Lindblad, S.; Sethio, D.; Berryman, O. B.; Erdélyi, M. Modulating photoswitch performance with halogen, coordinative and hydrogen bonding: a comparison of relative bond strengths. *Chem. Commun.* **2021**, *57*, 6261−6263.
(12) Yokoyama, S.; Nishiwaki, N. Fluorescence Behavior of Bis(cyanostyryl)pyrrole Derivatives Depending on the Substituent Position of Cyano Groups in Solution and in Solid State. *J. Org. Chem.* **2019**, *84*, 1192−1200.
(13) Zhao, Q.; He, J.; Yang, W.; Zhang, H.; Lin, L.; Jin, F.; Zhan, Y. Aggregation-induced Emission Characteristics and Distinct Fluorescent Responses to External Pressure Stimuli Based on Dumbbell D-π-A-π-D Cyanostyrene Derivatives. *Tetrahedron* **2020**, *76*, 131675.
(14) Yang, W.; Liu, C.; Lu, S.; Du, J.; Gao, Q.; Zhang, R.; Liu, Y.; Yang, C. AIE-active Smart Cyanostyrene Luminogens: Polymorphism-dependent Multicolor Mechanochromism. *J. Mater. Chem. C* **2018**, *6*, 290−298.
(15) Wei, P.; Zhang, J.-X.; Zhao, Z.; Chen, Y.; He, X.; Chen, M.; Gong, J.; Sung, H. H.-Y.; Williams, I. D.; Lam, J. W. Y.; Tang, B. Z. Multiple yet Controllable Photoswitching in a Single AIEgen System. *J. Am. Chem. Soc.* **2018**, *140*, 1966−1975.
(16) Zhu, L.; Ang, C. Y.; Li, X.; Nguyen, K. T.; Tan, S. Y.; Ågren, H.; Zhao, Y. Luminescent Color Conversion on Cyanostilbene-functionalized Quantum Dots via In-situ Photo-tuning. *Adv. Mater.* **2012**, *24*, 4020−4024.
(17) Zhu, L.; Li, X.; Zhang, Q.; Ma, X.; Li, M.; Zhang, H.; Luo, Z.; Ågren, H.; Zhao, Y. Unimolecular Photoconversion of Multicolor Luminescence on HierarchicalSelf-assemblies. *J. Am. Chem. Soc.* **2013**, *135*, 5175−5182.
(18) Fihey, A.; Perrier, A.; Browne, W. R.; Jacquemin, D. Multiphotochromic Molecular Systems. *Chem. Soc. Rev.* **2015**, *44*, 3719−3759.
(19) Liu, Z.; Dai, X.; Xu, Q.; Sun, X.; Liu, Y. Fluorescence Sensing of Glutathione Thiyl Radical by BODIPY-Modified β-Cyclodextrin. *Chin. J. Chem.* **2022**, *40*, 493−499.
(20) Liu, Z.; Dai, X.; Sun, Y.; Liu, Y. Organic Supramolecular Aggregates Based on Water-soluble Cyclodextrins and Calixarenes. *Aggregate* **2020**, *1*, 31−44.
(21) Chen, X.-Y.; Chen, H.; Đorđević, L.; Guo, Q.-H.; Wu, H.; Wang, Y.; Zhang, L.; Jiao, Y.; Cai, K.; Chen, H.; Stern, C. L.; Stupp, S. I.; Snurr, R. Q.; Shen, D.; Stoddart, J. F. Selective Photodimerization in a Cyclodextrin Metal-Organic Framework. *J. Am. Chem. Soc.* **2021**, *143*, 9129−9139.
(22) Wang, C.-Y.; Lou, X.-Y.; Cai, Z.; Zhang, M.-Z.; Jia, C.; Qin, J.-C.; Yang, Y.-W. Supramolecular Nanoplatform Based on Mesoporous Silica Nanocarriers and Pillararene Nanogates for Fungus Control. *ACS Appl. Mater. Interfaces* **2021**, *13*, 32295−32306.
(23) Yang, X.; Wang, R.; Kermagoret, A.; Bardelang, D. Oligomeric Cucurbituril Complexes: from Peculiar Assemblies to Emerging Applications. *Angew. Chem., Int. Ed.* **2020**, *59*, 21280−21292.
(24) Xu, D.-A.; Zhou, Q.-Y.; Dai, X.; Ma, X.-K.; Zhang, Y.-M.; Xu, X.; Liu, Y. Cucurbit[8]uril-mediated PhosphoresCent Supramolecular Foldamer for Antibiotics Sensing in Water and Cells. *Chin. Chem. Lett.* **2022**, *33*, 851−854.
(25) Fernandes, R. J.; Remón, P.; Moro, A. J.; Seco, A.; Ferreira, A. S. D.; Pischel, U.; Basílio, N. Toward Light-Controlled Supramolecular Peptide Dimerization. *J. Org. Chem.* **2021**, *86*, 8472−8478.
(26) Garain, S.; Garain, B. C.; Eswaramoorthy, M.; Pati, S. K.; George, S. J. Light-Harvesting Supramolecular Phosphors: Highly Efficient Room Temperature Phosphorescence in Solution and Hydrogels. *Angew. Chem., Int. Ed.* **2021**, *60*, 19720−19724.
(27) Kang, Y.; Tang, X.; Yu, H.; Cai, Z.; Huang, Z.; Wang, D.; Xu, J.-F.; Zhang, X. Supramolecular Catalyst Functions in Catalytic Amount: Cucurbit[8]uril Accelerates the Photodimerization of Brooker's Merocyanine. *Chem. Sci.* **2017**, *8*, 8357−8361.
(28) Wei, P.; Li, Z.; Zhang, J.-X.; Zhao, Z.; Xing, H.; Tu, Y.; Gong, J.; Cheung, T. S.; Hu, S.; Sung, H. H.-Y.; Williams, I. D.; Kwok, R. T. K.; Lam, J. W. Y.; Tang, B. Z. Molecular Transmission: Visible and Rate-Controllable Photoreactivity and Synergy of Aggregation-Induced Emission and Host−Guest Assembly. *Chem. Mater.* **2019**, *31*, 1092−1100.
(29) Zhao, N.; Li, P.; Zhuang, J.; Liu, Y.; Xiao, Y.; Qin, R.; Li, N. Aggregation-Induced Emission Luminogens with the Capability of Wide Color Tuning, Mitochondrial and Bacterial Imaging, and Photodynamic Anticancer and Antibacterial Therapy. *ACS Appl. Mater. Interfaces* **2019**, *11*, 11227−11237.
(30) Kim, H.-J.; Nandajan, P. C.; Gierschner, J.; Park, S. Y. Light-Harvesting Fluorescent Supramolecular Block Copolymers Based on Cyanostilbene Derivatives and Cucurbit[8]urils in Aqueous Solution. *Adv. Funct. Mater.* **2018**, *28*, 1705141.
(31) Kim, H.-J.; Whang, D. R.; Gierschner, J.; Park, S. Y. Highly Enhanced Fluorescence of Supramolecular Polymers Based on a Cyanostilbene Derivative and Cucurbit[8]uril in Aqueous Solution. *Angew. Chem., Int. Ed.* **2016**, *55*, 15915−15919.
(32) Kern, N.; Plesniak, M. P.; McDouall, J. J. W.; Procter, D. J. Enantioselective cyclizations and cyclization cascades of samarium ketyl radicals. *Nat. Chem.* **2017**, *9*, 1198−1204.
(33) Pusch, S.; Schollmeyer, D.; Opatz, T. A Light-Induced Vinylogous Nazarov-Type Cyclization. *Org. Lett.* **2016**, *18*, 3043−3045.
(34) Liu, S.; Ruspic, C.; Mukhopadhyay, P.; Chakrabarti, S.; Zavalij, P. Y.; Isaacs, L. The Cucurbit[n]uril Family: Prime Components for Self-Sorting Systems. *J. Am. Chem. Soc.* **2005**, *127*, 15959−15967.

https://doi.org/10.1021/acs.joc.2c00185
J. Org. Chem. XXXX, XXX, XXX−XXX